

New limits on dark matter annihilation from AMS cosmic ray positron data

Lars Bergström,^{1,*} Torsten Bringmann,^{2,†} Ilias Cholis,^{3,‡} Dan Hooper,^{3,4,§} and Christoph Weniger^{5,¶}

¹*The Oskar Klein Centre for Cosmoparticle Physics, Department of Physics,
Stockholm University, AlbaNova, SE-106 91 Stockholm, Sweden*

²*II. Institute for Theoretical Physics, University of Hamburg,
Luruper Chaussee 149, DE-22761 Hamburg, Germany*

³*Center for Particle Astrophysics, Fermi National Accelerator Laboratory, Batavia, IL 60510, USA*

⁴*University of Chicago, Department of Astronomy and Astrophysics, Chicago, Illinois, 60637, USA*

⁵*GRAPPA Institute, University of Amsterdam, Science Park 904, 1090 GL Amsterdam, Netherlands*

(Dated: October 25, 2013)

The AMS experiment onboard the International Space Station has recently provided cosmic ray electron and positron data with unprecedented precision in the range from 0.5 to 350 GeV. The observed rise in the positron fraction at energies above 10 GeV remains unexplained, with proposed solutions ranging from local pulsars to TeV-scale dark matter. Here, we make use of this high quality data to place stringent limits on dark matter with masses below ~ 300 GeV, annihilating or decaying to leptonic final states, essentially independent of the origin of this rise. We significantly improve on existing constraints, in some cases by up to two orders of magnitude.

PACS numbers: 95.85.Ry, 95.35.+d, 95.30.Cq; FERMILAB-PUB-13-202-A

Introduction. The AMS (Alpha Magnetic Spectrometer) collaboration has very recently announced the results of its first data collected from the International Space Station [1], consisting of a high precision measurement of the cosmic ray (CR) positron fraction [2]. This new data provides a confirmation of the rise of this quantity above 10 GeV, as previously observed by PAMELA [3] and Fermi [4] (and with earlier hints provided by HEAT [5] and AMS-01 [6]). Such a rise is not predicted in the standard scenario, in which CR positrons are mostly produced as *secondary* particles, as a result of collisions of CR protons with the interstellar medium (ISM). Instead, the large positron fraction seems to require the existence of at least one additional nearby *primary* source of high energy positrons. Local pulsars have emerged as the leading astrophysical candidates [7, 8], although it has also been argued that strong local sources might not actually be needed when taking into account the spiral structure of the Milky Way in full 3-D propagation models [9] and that even a secondary production mechanism in the shock waves of supernovae remnants [10, 11] could provide a viable mechanism to explain the data [12].

A more exotic possibility is that the observed positrons may be produced in the annihilations or decays of TeV-scale dark matter (DM) particles. Such scenarios, however, require unexpectedly large annihilation rates into predominantly leptonic final states [13–17] and are subject to significant constraints from CR antiproton, gamma-ray and synchrotron data [18–25]. Upcoming AMS data may help to settle this open issue not only by

increasing statistics and extending their study to higher energies, but also by providing high precision measurements of other CR particle spectra (likely breaking degeneracies in the propagation parameters [26]). Fermi and AMS will also further constrain any anisotropy in the positron/electron flux (where current limits are already close to discriminating between some of the scenarios described above [27, 28]).

In this Letter, we do not make any attempt to explain the origin of the rise in the positron fraction. Instead, we focus on using the AMS data to derive limits on subdominant exotic contributions to the observed CR positron spectrum, in particular from DM with masses below ~ 300 GeV. While positrons have been used in the past to probe DM annihilation or decay [29–34], we exploit here for the first time the extremely high quality of the AMS data to search for pronounced *spectral features* in the positron flux predicted in some DM models [35–41]. Much as exploiting spectral features can significantly improve the sensitivity of indirect DM searches using gamma rays [42], we demonstrate that the same is true for positrons, despite energy losses and other complicating factors. We derive limits that exceed the currently most stringent results on DM annihilation into leptons [43, 44] by up to two orders of magnitude.

This Letter is organized as follows. We first briefly review various astrophysical sources of leptons and how they manifest themselves in the observed CR flux, and then discuss possible contributions from DM. We continue with a description of the statistical treatment implemented here, before moving on to present our main results and conclusions. In an Appendix [45], we collect further technical details of our procedure for deriving limits on a possible DM signal, discussing in particular the impact of systematic uncertainties in the background modeling.

* lbe@fysik.su.se

† torsten.bringmann@desy.de

‡ cholis@fnal.gov

§ dhooper@fnal.gov

¶ c.weniger@uva.nl

Astrophysical origins of cosmic ray leptons. The origin of high energy electrons can be traced back to i) supernova explosions that accelerate the ISM to produce what are typically referred to as primary CRs, ii) inelastic collisions of primary CR protons and nuclei with the ISM (resulting in charged mesons, which decay, producing secondary electrons *and* positrons), and iii) individual sources such as pulsars that produce e^\pm pairs. The averaged spectrum of propagated primary CR electrons (originating from many supernovae) is expected to be harder than that of the secondary e^\pm component because the primary CR progenitors of the secondaries have also experienced propagation effects; both spectra are well described by power-laws, with spectral indices of about 3.3 to 3.5 (3.7) for primary electrons (secondary e^\pm) at energies above ~ 10 GeV [46]. The contribution from all galactic pulsars can be approximated by a power-law with an exponential cut-off at high energies, with a propagated spectral index of 2.0 ± 0.5 [7, 8].

The Galactic Magnetic Field at scales $\gtrsim 100$ pc has a random and a regular component [47]. As CR leptons propagate away from their sources, they follow the field lines and scatter off B -field irregularities. The net effect can be approximated as a random walk diffusion within a zone surrounding the Galactic Disk [48, 49]. Further away from the disk the magnetic fields become weak, essentially leading to freely propagating CRs. During their propagation throughout the Galaxy, electrons and positrons also experience significant energy losses due to synchrotron and inverse Compton scattering on the galactic radiation field and the cosmic microwave background. The impact of other effects such as convective winds, ionization losses, or positron annihilation in collisions with matter are not significant for leptons in the energy range considered here [49, 50] and are therefore ignored. We do, however, include bremsstrahlung emission, diffusive re-acceleration, and solar modulation inside the heliosphere (using the force-field approximation [51]), which have an impact on CR e^\pm spectra below 5–10 GeV [52, 53].

For the propagation of CR leptons, we use the standard numerical tool GALPROP v54 [54], which includes up-to-date implementations of the local interstellar radiation field and galactic gas distribution. These are relevant for both the production of secondary leptons and energy losses. GALPROP assumes a diffusion zone with cylindrical symmetry within which CRs diffuse and beyond which they escape. Its scale height, L , and other diffusion parameters, notably the diffusion time-scale and local diffusion properties, are constrained by observed CR ratios, including \bar{p}/p , B/C and $^{10}\text{Be}/^9\text{Be}$. As reference values we assume $L = 4$ kpc, corresponding to the value best-fit by CR data [55] and favored by radio observations [56], and the standard default GALPROP assumptions for the local radiation and magnetic field energy densities, corresponding to $U_{\text{rad}} + U_B = 1.7 \text{ eV cm}^{-3}$ [54]. For the diffusion zone scale height, values of $L < 2$ kpc are in tension with a combined analysis of CR and gamma-ray data [57],

while increasing L beyond 8 kpc does not significantly alter our results.¹ The propagation of high-energy leptons is actually dominated by energy losses rather than diffusion, implying that more conservative limits would arise for larger values of the local radiation and magnetic field energy densities. In our subsequent discussion, we will allow for an increase of $U_{\text{rad}} + U_B$ by up to 50% with respect to the reference value, which is still compatible with gamma-ray and synchrotron data [56, 58].

Positrons from dark matter. DM particles annihilating or decaying in the Galactic Halo may also contribute to the CR lepton spectrum, producing equal numbers of positrons and electrons. For annihilating DM, the injected spectrum of CR leptons per volume and time is given by $Q = \frac{1}{2} \langle \sigma v \rangle (\rho_\chi / m_\chi)^2 dN/dE$ (divided by 2 if the DM particle is not self-conjugate), while for decaying DM, this is instead $Q = \Gamma \rho_\chi / m_\chi dN/dE$, where Γ is the decay rate. Here, $\langle \sigma v \rangle$ is the velocity-averaged annihilation rate, ρ_χ is the DM density, m_χ is the DM mass, and dN/dE is the spectrum of leptons produced per annihilation or decay. As our default choice, we adopt a DM distribution which follows an Einasto profile [59], normalized to a local density of $\rho_\chi^\odot = 0.4 \text{ GeV}$ [60, 61].

Positrons from DM annihilation or decay typically result from the decay of π^+ (for hadronic final states), or the leptonic decay of τ^+ or μ^+ . Owing to the high multiplicity of such processes, the resulting e^+ energy distribution at injection (which we take from Ref. [62]) is typically very soft. If DM annihilates directly into e^\pm , however, these are produced nearly monochromatically. Even after accounting for energy losses from propagation, a very characteristic spectrum arises in this case, with a sharp edge-like feature at $E = m_\chi$ (or at $E = m_\chi/2$ for decaying DM). A comparably distinct spectral feature arises from the annihilation of Majorana DM into $e^+e^-\gamma$ final states. Popular examples for DM models with large annihilation rates into e^\pm final states include Kaluza-Klein DM [38], while the supersymmetric neutralino is a possible candidate for producing a spectrum dominated by $e^+e^-\gamma$ final states [40].²

We illustrate this in Fig. 1 by showing the propagated e^\pm spectra for various final states and an annihilation rate that corresponds to the “thermal” cross section of $\langle \sigma v \rangle_{\text{therm}} \equiv 3 \times 10^{-26} \text{ cm}^3 \text{ s}^{-1}$ (which leads to the correct relic density in the simplest models of thermally produced DM). As anticipated, the e^+e^- and $e^+e^-\gamma$ final states result in the most pronounced spectral features – a fact which helps considerably, as we will see, to distinguish them from astrophysical backgrounds. For the case of e^+e^- final states, we also show how the spectrum

¹ For $L = 2, 4, 8$ kpc and rigidity R , we adopt a diffusion coefficient $D(R) = D_0 (\frac{R}{1 \text{ GV}})^{0.5}$, with $D_0 = 0.81, 1.90, 2.65$ ($\times 10^{28} \text{ cm}^2 \text{ s}^{-1}$), and Alfvén velocities 9, 10, 10 km s^{-1} .

² By $e^+e^-\gamma$ we will always refer to that specific situation, dominated by photon emission off virtual selectrons \tilde{e} . We assume at least one of the \tilde{e} to be degenerate in mass with the neutralino.

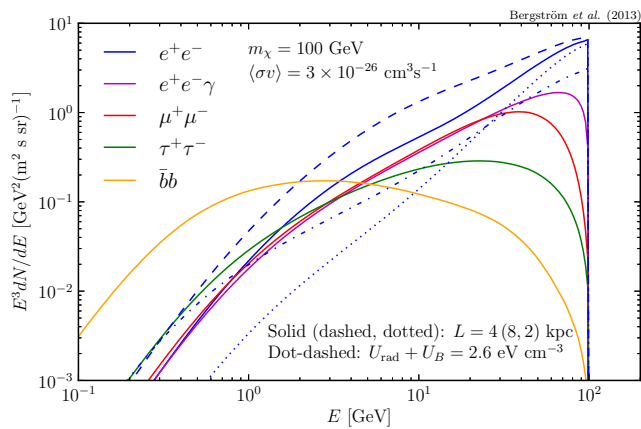


FIG. 1. The e^\pm spectrum from annihilating DM, after propagation, for different annihilation final states, assuming $\langle\sigma v\rangle = 3 \times 10^{-26} \text{ cm}^3\text{s}^{-1}$. Solid lines refer to reference diffusion zone ($L=4$ kpc) and energy loss assumptions ($U_{\text{rad}} + U_B = 1.7 \text{ eV cm}^{-3}$). Dashed (dotted) lines show the effect of a different scale height $L=8$ (2) kpc. The dash-dotted line shows the impact of increasing the local radiation plus magnetic field density to $U_{\text{rad}} + U_B = 2.6 \text{ eV cm}^{-3}$.

depends on our local diffusion and energy loss assumptions within the range discussed above. Increasing L enables CR leptons to reach us from greater distances due to the larger diffusion volume and therefore results in softer propagated spectra. While the peak normalization of the spectrum depends only marginally on L , it may be reduced by up to a factor of ~ 2 when increasing the assumed local energy losses via synchrotron radiation and inverse Compton scattering by 50%. In Fig. 2, we show a direct comparison of the DM signal with the AMS data, for the case of e^+e^- final states contributing at the maximum level allowed by our constraints (see below) for two fiducial values of m_χ . Again, it should be obvious that the shape of the DM contribution differs at all energies significantly from that of the background.

Statistical treatment. We use the likelihood ratio test [63] to determine the significance of, and limits on, a possible DM contribution to the positron fraction measured by AMS. As likelihood function, we adopt a product of normal distributions $\mathcal{L} = \prod_i N(f_i|\mu_i, \sigma_i)$; f_i is the measured value, μ_i the positron fraction predicted by the model, and σ_i its variance. The DM contribution enters with a single degree of freedom, given by the non-negative signal normalization. Upper limits at the 95%CL on the DM annihilation or decay rate are therefore derived by increasing the signal normalization from its best-fit value until $-2 \ln \mathcal{L}$ is changed by 2.71, while profiling over the parameters of the background model.

We use data in the energy range 1–350 GeV; the variance σ_i is approximated by adding the statistical and systematic errors of the measurement in quadrature, $\sigma_i = (\sigma_{i,\text{stat}}^2 + \sigma_{i,\text{sys}}^2)^{1/2}$. Since the total relative error is always small (below 17%), and at energies above 4 GeV dominated by statistics, we expect this approximation to

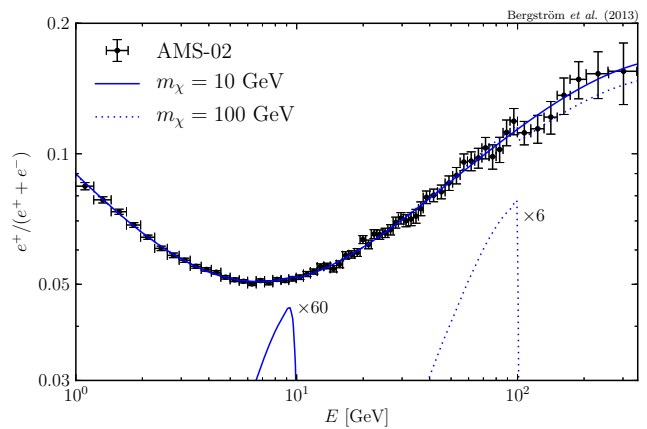


FIG. 2. The AMS positron fraction measurement [2] and background+signal fit for DM annihilating directly to e^+e^- , for $m_\chi = 10$ GeV and 100 GeV. The normalization of the DM signal in each case was chosen such that it is barely excluded at the 95% CL. For better visibility, the contribution from DM (lower lines) has been rescaled as indicated.

be very reliable. The binning of the published positron fraction follows the AMS energy resolution, which varies between 10.4% at 1 GeV and 1.5% at 350 GeV. Although we do not account for the finite energy resolution of AMS in our analysis, we have explicitly checked that this impacts our results by no more than 10%.

As our nominal model for the part of the e^\pm spectrum that does not originate from DM, henceforth simply referred to as the astrophysical background, we use the same phenomenological parameterization as the AMS collaboration in their analysis [2]. This parameterization describes each of the e^\pm fluxes as the sum of a common source spectrum – modeled as a power-law with exponential cutoff – and an individual power-law contribution (only the latter being different for the e^+ and e^- fluxes). After adjusting normalization and slope of the secondary positrons such that the overall flux reproduces the Fermi $e^+ + e^-$ measurements [64], the five remaining model parameters are left unconstrained. This phenomenological parameterization provides an extremely good fit (with a $\chi^2/\text{d.o.f.} = 28.5/57$), indicating that no fine structures are observed in the AMS data. For the best-fit spectral slopes of the individual power-laws we find $\gamma_{e^-} \simeq 3.1$ and $\gamma_{e^+} \simeq 3.8$, respectively, and for the common source $\gamma_{e^\pm} \simeq 2.5$ with a cutoff at $E_c \simeq 800$ GeV, consistent with Ref. [2]. Subsequently, we will keep E_c fixed to its best-fit value.

Results and Discussion. Our main results are the bounds on the DM annihilation cross section, as shown in Fig. 3. No significant excess above background was observed. For annihilations proceeding entirely to e^+e^- final states, we find that the “thermal” cross section is firmly excluded for $m_\chi \lesssim 90$ GeV. For $m_\chi \sim 10$ GeV, which is an interesting range in light of recent results from direct [65–69] and indirect [70–72] DM searches,

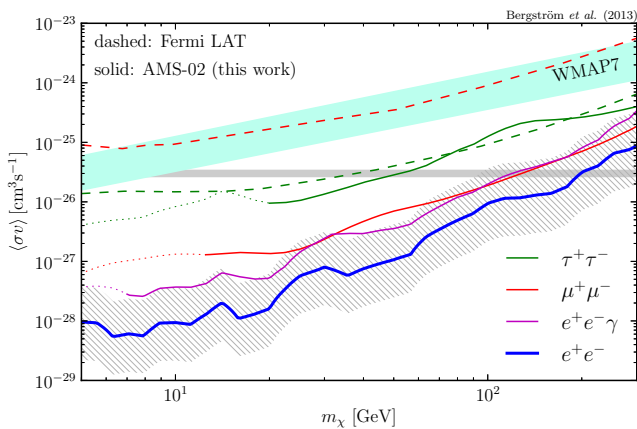


FIG. 3. Upper limits (95% CL) on the DM annihilation cross section, as derived from the AMS positron fraction, for various final states (this work), WMAP7 (for $\ell^+\ell^-$) [44] and Fermi LAT dwarf spheroidals (for $\mu^+\mu^-$ and $\tau^+\tau^-$) [43]. The dotted portions of the curves are potentially affected by solar modulation. We also indicate $\langle\sigma v\rangle_{\text{therm}} \equiv 3 \times 10^{-26} \text{ cm}^3\text{s}^{-1}$. The AMS limits are shown for reasonable reference values of the local DM density and energy loss rate (see text), and can vary by a factor of a few, as indicated by the hatched band (for clarity, this band is only shown around the e^+e^- constraint).

our upper bound on the annihilation cross section to e^+e^- is approximately two orders of magnitude below $\langle\sigma v\rangle_{\text{therm}}$. If only a fraction f of DM annihilates like assumed, limits would scale like f^{-2} (and, very roughly, $\langle\sigma v\rangle_{\text{therm}} \propto f^{-1}$). We also show in Fig. 3 the upper bounds obtained for other leptonic final states. As expected, these limits are weaker than those found in the case of direct annihilation to electrons – both because part of the energy is taken away by other particles (neutrinos, in particular) and because they feature broader and less distinctive spectral shapes. These new limits on DM annihilating to $\mu^+\mu^-$ and $\tau^+\tau^-$ final states are still, however, highly competitive with or much stronger than those derived from other observations, such as from the cosmic microwave background [44] and from gamma-ray observations of dwarf galaxies [43]. Note that for the case of $e^+e^-\gamma$ final states even stronger limits can be derived for $m_\chi \gtrsim 50 \text{ GeV}$ by a spectral analysis of gamma rays [73]. We do not show results for the $b\bar{b}$ channel, for which we nominally find even weaker limits due to the broader spectrum (for $m_\chi \simeq 100 \text{ GeV}$, about $\langle\sigma v\rangle \lesssim 1.1 \cdot 10^{-24} \text{ cm}^3\text{s}^{-1}$). In fact, due to degeneracies with the background modeling, limits for annihilation channels which produce such a broad spectrum of positrons can suffer from significant systematic uncertainties. For this reason, we consider our limits on the e^+e^- channel to be the most robust.

Uncertainties in the e^\pm energy loss rate and local DM density weaken, to some extent, our ability to robustly constrain the annihilation cross sections under consideration in Fig. 3. We reflect this uncertainty by show-

ing a band around the e^+e^- constraint, corresponding to the range $U_{\text{rad}} + U_B = (1.2 - 2.6) \text{ eV cm}^{-3}$, and $\rho_\chi^\odot = (0.25 - 0.7) \text{ GeV cm}^{-3}$ [61, 74] (note that the form of the DM profile has a much smaller impact). Uncertainty bands of the same width apply to each of the other final states shown in the figure, but are not explicitly shown for clarity. Other diffusion parameter choices impact our limits only by up to $\sim 10\%$, except for the case of low DM masses, for which the effect of solar modulation may be increasingly important [53, 75]. We reflect this in Fig. 3 by depicting the limits derived in this less certain mass range, where the peak of the signal e^+ flux (as shown in Fig. 1) falls below a fiducial value of 5 GeV, with dotted rather than solid lines.

For comparison, we have also considered a collection of physical background models in which we calculated the expected primary and secondary lepton fluxes using GALPROP, and then added the contribution from all galactic pulsars. While this leads to an almost identical description of the background at high energies as in the phenomenological model, small differences are manifest at lower energies due to solar modulation and a spectral break [55, 76, 77] in the CR injection spectrum at a few GeV (both neglected in the AMS parameterization). We cross-check our fit to the AMS positron fraction with lepton measurements by Fermi [64]. Using these physical background models in our fits, instead of the phenomenological AMS parameterization, the limits do not change significantly. The arguably most extreme case would be the appearance of dips in the background due to the superposition of several pulsar contributions, which might conspire with a hidden DM signal at almost exactly the same energy. We find that in such situations, the real limits on the annihilation rate could be weaker (or stronger) by up to roughly a factor of 3 for any individual value of m_χ . See the Appendix [45] for more details and further discussion of possible systematics that might affect our analysis.

Lastly, we note that the upper limits on $\langle\sigma v\rangle(m_\chi)$ reported in Fig. 3 can easily be translated into upper limits on the decay width of a DM particle of mass $2m_\chi$ via $\Gamma \simeq \langle\sigma v\rangle\rho_\chi^\odot/m_\chi$. We checked explicitly that this simple transformation is correct to better than 10% for the $L=4 \text{ kpc}$ propagation scenario and e^+e^- and $\mu^+\mu^-$ final states over the full considered energy range.

Conclusions. In this Letter, we have considered a possible dark matter contribution to the recent AMS cosmic ray positron fraction data. The high quality of this data has allowed us for the first time to successfully perform a spectral analysis, similar to that used previously in the context of gamma ray searches for DM. While we have found no indication of a DM signal, we have derived upper bounds on annihilation and decay rates into leptonic final states that improve upon the most stringent current limits by up to two orders of magnitude. For light DM in particular, our limits for e^+e^- and $\mu^+\mu^-$ final states are significantly below the cross section naively predicted for a simple thermal relic. When taken together

with constraints on DM annihilations to hadronic final states from gamma rays [43] and antiprotons [22], this new information significantly limits the range of models which may contain a viable candidate for dark matter with $m_\chi \sim \mathcal{O}(10)$ GeV.

The AMS mission is planned to continue for 20 years. Compared to the 18 months of data [2] our analysis is based on, we expect to be able to strengthen the presented limits by at least a factor of three in the energy range of 6–200 GeV with the total data set, and by more in the likely case that systematics and the effective ac-

ceptance of the instrument improve.

ACKNOWLEDGMENTS

This work makes use of SciPy [78], Minuit [79] and Matplotlib [80]. The research of L.B. was carried out under Swedish Research Council (VR) contract no. 621-2009-3915. T.B. acknowledges support from the German Research Foundation (DFG) through the Emmy Noether grant BR 3954/1-1. I.C., C.W. and D.H. thank the *Kavli Institute for Theoretical Physics* in Santa Barbara, California, for their kind hospitality. This work has been supported by the US Department of Energy.

-
- [1] www.ams02.org
- [2] M. Aguilar *et al.* [AMS Collaboration], Phys. Rev. Lett. **110**, no. 14, 141102 (2013).
- [3] O. Adriani *et al.* [PAMELA Collaboration], Nature **458**, 607 (2009) [arXiv:0810.4995 [astro-ph]].
- [4] M. Ackermann *et al.* [Fermi LAT Collaboration], Phys. Rev. Lett. **108**, 011103 (2012) [arXiv:1109.0521 [astro-ph.HE]].
- [5] S. W. Barwick *et al.* [HEAT Collaboration], Astrophys. J. **482**, L191 (1997) [astro-ph/9703192].
- [6] M. Aguilar *et al.* [AMS-01 Collaboration], Phys. Lett. B **646**, 145 (2007) [astro-ph/0703154 [ASTRO-PH]].
- [7] D. Hooper, P. Blasi and P. D. Serpico, JCAP **0901**, 025 (2009) [arXiv:0810.1527 [astro-ph]].
- [8] S. Profumo, Central Eur. J. Phys. **10**, 1 (2011) [arXiv:0812.4457 [astro-ph]].
- [9] D. Gaggero, L. Maccione, G. Di Bernardo, C. Evoli and D. Grasso, Phys. Rev. Lett. **111**, 021102 (2013) [arXiv:1304.6718 [astro-ph.HE]].
- [10] P. Blasi, Phys. Rev. Lett. **103**, 051104 (2009) [arXiv:0903.2794 [astro-ph.HE]].
- [11] P. Mertsch and S. Sarkar, Phys. Rev. Lett. **103**, 081104 (2009) [arXiv:0905.3152 [astro-ph.HE]].
- [12] For a review, see P. D. Serpico, Astropart. Phys. **39-40**, 2 (2012) [arXiv:1108.4827 [astro-ph.HE]].
- [13] L. Bergström, J. Edsjö and G. Zaharijas, Phys. Rev. Lett. **103**, 031103 (2009) [arXiv:0905.0333 [astro-ph.HE]].
- [14] D. P. Finkbeiner, L. Goodenough, T. R. Slatyer, M. Vogelsberger and N. Weiner, JCAP **1105**, 002 (2011) [arXiv:1011.3082 [hep-ph]].
- [15] Q. Yuan, X. -J. Bi, G. -M. Chen, Y. -Q. Guo, S. -J. Lin and X. Zhang, arXiv:1304.1482 [astro-ph.HE].
- [16] I. Cholis and D. Hooper, Phys. Rev. D **88**, 023013 (2013) [arXiv:1304.1840 [astro-ph.HE]].
- [17] H. -B. Jin, Y. -L. Wu and Y. -F. Zhou, arXiv:1304.1997 [hep-ph].
- [18] F. Donato, D. Maurin, P. Brun, T. Delahaye and P. Salati, Phys. Rev. Lett. **102**, 071301 (2009) [arXiv:0810.5292 [astro-ph]].
- [19] G. Bertone, M. Cirelli, A. Strumia and M. Taoso, JCAP **0903**, 009 (2009) [arXiv:0811.3744 [astro-ph]].
- [20] L. Bergström, G. Bertone, T. Bringmann, J. Edsjö and M. Taoso, Phys. Rev. D **79**, 081303 (2009) [arXiv:0812.3895 [astro-ph]].
- [21] M. Cirelli, P. Panci and P. D. Serpico, Nucl. Phys. B **840**, 284 (2010) [arXiv:0912.0663 [astro-ph.CO]].
- [22] C. Evoli, I. Cholis, D. Grasso, L. Maccione and P. Ullio, Phys. Rev. D **85**, 123511 (2012) [arXiv:1108.0664 [astro-ph.HE]].
- [23] R. Kappl and M. W. Winkler, Phys. Rev. D **85**, 123522 (2012) [arXiv:1110.4376 [hep-ph]].
- [24] M. Wechakama and Y. Ascasibar, arXiv:1212.2583 [astro-ph.CO].
- [25] A. De Simone, A. Riotto and W. Xue, JCAP **1305**, 003 (2013) [arXiv:1304.1336 [hep-ph]].
- [26] M. Pato, D. Hooper and M. Simet, JCAP **1006**, 022 (2010) [arXiv:1002.3341 [astro-ph.HE]].
- [27] M. Ackermann *et al.* [Fermi-LAT Collaboration], Phys. Rev. D **82**, 092003 (2010) [arXiv:1008.5119 [astro-ph.HE]].
- [28] G. Di Bernardo, C. Evoli, D. Gaggero, D. Grasso, L. Maccione and M. N. Mazziotta, Astropart. Phys. **34**, 528 (2011) [arXiv:1010.0174 [astro-ph.HE]].
- [29] J. R. Ellis, R. A. Flores, K. Freese, S. Ritz, D. Seckel and J. Silk, Phys. Lett. B **214**, 403 (1988).
- [30] S. Rudaz and F. W. Stecker, Astrophys. J. **325**, 16 (1988).
- [31] M. Kamionkowski and M. S. Turner, Phys. Rev. D **43**, 1774 (1991).
- [32] E. A. Baltz and J. Edsjö, Phys. Rev. D **59**, 023511 (1998) [astro-ph/9808243].
- [33] E. A. Baltz, J. Edsjö, K. Freese and P. Gondolo, Phys. Rev. D **65**, 063511 (2002) [astro-ph/0109318].
- [34] J. Kopp, arXiv:1304.1184 [hep-ph].
- [35] A. J. Tylka, Phys. Rev. Lett. **63**, 840 (1989) [Erratum-ibid. **63**, 1658 (1989)].
- [36] M. S. Turner and F. Wilczek, Phys. Rev. D **42**, 1001 (1990).
- [37] E. A. Baltz and L. Bergström, Phys. Rev. D **67**, 043516 (2003) [hep-ph/0211325].
- [38] D. Hooper and G. D. Kribs, Phys. Rev. D **70**, 115004 (2004) [hep-ph/0406026].
- [39] E. A. Baltz and D. Hooper, JCAP **0507**, 001 (2005) [hep-ph/0411053].
- [40] L. Bergström, T. Bringmann and J. Edsjö, Phys. Rev. D **78**, 103520 (2008) [arXiv:0808.3725 [astro-ph]].
- [41] D. Hooper and W. Xue, Phys. Rev. Lett. **110**, 041302 (2013) [arXiv:1210.1220 [astro-ph.HE]].

- [42] T. Bringmann, F. Calore, G. Vertongen and C. Weniger, *Phys. Rev. D* **84**, 103525 (2011) [arXiv:1106.1874 [hep-ph]].
- [43] M. Ackermann *et al.* [Fermi-LAT Collaboration], *Phys. Rev. Lett.* **107**, 241302 (2011) [arXiv:1108.3546 [astro-ph.HE]].
- [44] S. Galli, F. Iocco, G. Bertone and A. Melchiorri, *Phys. Rev. D* **80**, 023505 (2009) [arXiv:0905.0003 [astro-ph.CO]]; T. R. Slatyer, N. Padmanabhan and D. P. Finkbeiner, *Phys. Rev. D* **80**, 043526 (2009) [arXiv:0906.1197 [astro-ph.CO]]; S. Galli, F. Iocco, G. Bertone and A. Melchiorri, *Phys. Rev. D* **84**, 027302 (2011) [arXiv:1106.1528 [astro-ph.CO]]; T. R. Slatyer, arXiv:1211.0283 [astro-ph.CO]; J. M. Cline and P. Scott, *JCAP* **1303**, 044 (2013) [Erratum-ibid. **1305**, E01 (2013)] [arXiv:1301.5908 [astro-ph.CO]]; L. Lopez-Honorez, O. Mena, S. Palomares-Ruiz and A. C. Vincent, *JCAP* **1307**, 046 (2013) [arXiv:1303.5094 [astro-ph.CO]].
- [45] See Appendix.
- [46] See, e.g., I. V. Moskalenko and A. W. Strong, *Astrophys. J.* **493**, 694 (1998) [astro-ph/9710124]; R. Schlickeiser, "Cosmic Ray Astrophysics" Springer (2002), and references therein. For an alternative discussion, see also B. Katz, K. Blum and E. Waxman, *Mon. Not. Roy. Astron. Soc.* **405**, 1458 (2010) [arXiv:0907.1686 [astro-ph]].
- [47] See R. Jansson, G. R. Farrar, A. H. Waelkens and T. A. Ensslin, *JCAP* **0907**, 021 (2009) [arXiv:0905.2228[astro-ph]]. and references therein.
- [48] M. S. Longair, "High Energy Astrophysics", Vol. **1** pp. 346-350, Cambridge University Press (2004).
- [49] A. W. Strong, I. V. Moskalenko and V. S. Ptuskin, *Ann. Rev. Nucl. Part. Sci.* **57**, 285 (2007) [astro-ph/0701517].
- [50] M. S. Longair, "High Energy Astrophysics", Vol. **2** pp. 274-286, Cambridge University Press (2004).
- [51] L. J. Gleeson and W. I. Axford, *Astrophys. J.* **154**, 1011 (1968).
- [52] R. D. Strauss, M. S. Potgieter, I. Büsching and A. Kopp, *Astrophys. J.* **735**, 83 (2011).
- [53] L. Maccione, *Phys. Rev. Lett.* **110**, 081101 (2013) [arXiv:1211.6905[astro-ph.HE]].
- [54] A. W. Strong, I. V. Moskalenko, T. A. Porter, E. Orlando, S. W. Digel and A. E. Vladimirov "GALPROP v.54: Explanatory Supplement (2011)"; <http://galprop.stanford.edu/>.
- [55] R. Trotta, G. Johannesson, I. V. Moskalenko, T. A. Porter, R. R. de Austri and A. W. Strong, *Astrophys. J.* **729**, 106 (2011) [arXiv:1011.0037[astro-ph.HE]].
- [56] T. Bringmann, F. Donato and R. A. Lineros, *JCAP* **1201**, 049 (2012) [arXiv:1106.4821 [astro-ph.GA]].
- [57] I. Cholis, M. Tavakoli, C. Evoli and P. Ullio, *JCAP* **1205**, 004 (2012) [arXiv:1106.5073[astro-ph.HE]].
- [58] T. R. Jaffe, A. J. Banday, J. P. Leahy, S. Leach and A. W. Strong, [arXiv:1105.5885[astro-ph.GA]].
- [59] D. Merritt, J. F. Navarro, A. Ludlow and A. Jenkins, *Astrophys. J.* **624**, L85 (2005) [astro-ph/0502515].
- [60] R. Catena and P. Ullio, *JCAP* **1008**, 004 (2010) [arXiv:0907.0018 [astro-ph.CO]].
- [61] P. Salucci, F. Nesti, G. Gentile and C. F. Martins, *Astron. Astrophys.* **523**, A83 (2010) [arXiv:1003.3101 [astro-ph.GA]].
- [62] M. Cirelli, G. Corcella, A. Hektor, G. Hutsi, M. Kadastik, P. Panci, M. Raidal and F. Sala *et al.*, *JCAP* **1103**, 051 (2011) [Erratum-ibid. **1210**, E01 (2012)] [arXiv:1012.4515 [hep-ph]].
- [63] W. A. Rolke, A. M. Lopez and J. Conrad, *Nucl. Instrum. Meth. A* **551**, 493 (2005) [physics/0403059].
- [64] M. Ackermann *et al.* [Fermi LAT Collaboration], *Phys. Rev. D* **82**, 092004 (2010) [arXiv:1008.3999 [astro-ph.HE]].
- [65] R. Bernabei *et al.* [DAMA and LIBRA Collaborations], *Eur. Phys. J. C* **67**, 39 (2010) [arXiv:1002.1028 [astro-ph.GA]].
- [66] C. E. Aalseth, P. S. Barbeau, J. Colaresi, J. I. Collar, J. Diaz Leon, J. E. Fast, N. Fields and T. W. Hossbach *et al.*, *Phys. Rev. Lett.* **107**, 141301 (2011) [arXiv:1106.0650 [astro-ph.CO]].
- [67] G. Angloher, M. Bauer, I. Bavykina, A. Bento, C. Bucci, C. Ciemiak, G. Deuter and F. von Feilitzsch *et al.*, *Eur. Phys. J. C* **72**, 1971 (2012) [arXiv:1109.0702 [astro-ph.CO]].
- [68] R. Agnese *et al.* [CDMS Collaboration], [arXiv:1304.4279 [hep-ex]].
- [69] M. T. Frandsen, F. Kahlhoefer, C. McCabe, S. Sarkar and K. Schmidt-Hoberg, *JCAP* **1307**, 023 (2013) [arXiv:1304.6066 [hep-ph]].
- [70] D. Hooper and T. Linden, *Phys. Rev. D* **84**, 123005 (2011) [arXiv:1110.0006 [astro-ph.HE]].
- [71] D. Hooper and T. R. Slatyer, arXiv:1302.6589 [astro-ph.HE].
- [72] K. N. Abazajian and M. Kaplinghat, *Phys. Rev. D* **86**, 083511 (2012) [arXiv:1207.6047 [astro-ph.HE]].
- [73] T. Bringmann, X. Huang, A. Ibarra, S. Vogl and C. Weniger, *JCAP* **1207**, 054 (2012) [arXiv:1203.1312 [hep-ph]].
- [74] F. Iocco, M. Pato, G. Bertone and P. Jetzer, *JCAP* **1111**, 029 (2011) [arXiv:1107.5810 [astro-ph.GA]].
- [75] S. Della Torre, P. Bobik, M. J. Boschini, C. Consolandi, M. Gervasi, D. Grandi, K. Kudela and S. Pensotti *et al.*, *Adv. Space Res.* **49**, 1587 (2012).
- [76] A. W. Strong, I. V. Moskalenko and O. Reimer, *Astrophys. J.* **537**, 763 (2000) [Erratum-ibid. **541**, 1109 (2000)] [astro-ph/9811296]; A. W. Strong, I. V. Moskalenko and O. Reimer, *Astrophys. J.* **613**, 962 (2004) [astro-ph/0406254].
- [77] V. S. Ptuskin, I. V. Moskalenko, F. C. Jones, A. W. Strong and V. N. Zirakashvili, *Astrophys. J.* **642**, 902 (2006) [astro-ph/0510335].
- [78] E. Jones, T. Oliphant, P. Peterson, *et al.*, *SciPy: Open source scientific tools for Python*, 2001.
- [79] F. James and M. Roos, *Comput. Phys. Commun.* **10**, 343 (1975).
- [80] J. D. Hunter, *Matplotlib: A 2D graphics environment*, *Comput. in Science & Engineering* **9**, 90 (2007).
- [81] O. Adriani, *et al.* [PAMELA Collaboration], *Phys. Rev. Lett.* **106**, 201101 (2011).
- [82] R. D. Strauss, M. S. Potgieter, I. Büsching and A. Kopp, *Astrophys. & Sp. Sc.* **339**, 223 (2012).
- [83] J. Arons, *Space Sci. Rev.* **75**, 235 (1996) [arXiv:0811.3894 [astro-ph]].
- [84] D. A. Green, [arXiv:0905.3699 [astro-ph]].
- [85] D. Malyshev, I. Cholis and J. Gelfand, *Phys. Rev. D* **80**, 063005 (2009) [arXiv:0903.1310 [astro-ph.HE]].
- [86] T. Kobayashi, Y. Komori, K. Yoshida and J. Nishimura, *Astrophys. J.* **601**, 340 (2004) [astro-ph/0308470 [astro-ph]].
- [87] D. Grasso *et al.* [Fermi-LAT Collaboration], *Astropart. Phys.* **32**, 140 (2009) [arXiv:0905.0636 [astro-ph.HE]].

- [88] R. N. Manchester, G. B. Hobbs, A. Teoh and M. Hobbs, *Astrophys. J.* **129**, 1993 (2005); <http://www.atnf.csiro.au/people/pulsar/psrcat/> .
- [89] P. Gondolo, J. Edsjö, P. Ullio, L. Bergström, M. Schelke and E. A. Baltz, *JCAP* **0407**, 008 (2004) [[astro-ph/0406204](http://arxiv.org/abs/astro-ph/0406204)]; P. Gondolo, J. Edsjö, L. Bergström, P. Ullio, M. Schelke, E. A. Baltz, T. Bringmann and G. Duda, <http://www.darksusy.org>.

[45] APPENDIX

Here, we describe additional tests carried out in order to estimate the degree to which our DM limits might vary under alternative assumptions pertaining to the astrophysical background and cosmic ray propagation. In addition, we quantify the significance of spectral features in the observed positron fraction.

In deriving our main results, as shown in Fig. 3, we used the phenomenological parameterization of the AMS collaboration [2] for the astrophysical contribution to the positron fraction, and adopted our reference assumptions of $L = 4$ kpc and $U_{rad} + U_B = 1.7$ eV cm⁻³. In Fig. 4, for the case of direct DM annihilation to e^+e^- , we show in the *left panel* the impact of different propagation parameters when treating the astrophysical background in the same way as in Fig. 3. Changing the diffusion conditions ($L = 2 - 8$ kpc) in the Galaxy in that case only affects our limits by $O(10\%)$, while allowing for higher energy losses ($U_{rad} + U_B = 2.6$ eV cm⁻³) can alter our limits by a factor of ~ 2 , with higher losses resulting in weaker limits (see also Fig. 1). In the *right panel*, we repeat this exercise, but replace the AMS background parametrization with physically motivated models for the primary e^- , secondary e^\pm , and pulsar originated e^\pm fluxes (see discussion in the main text), calculated with the same galactic propagation model as used in determining the spectrum of CR leptons from DM. In this case, our results can be further altered by a factor of up to ~ 3 . The reason for this change is that our physically motivated models describe the individual components by power-laws with breaks at a few GeV. These spectral features in the background can be the result of different energy loss mechanisms kicking in,³ or from individual local and recent supernovae affecting the high energy e^- spectrum. Also, observations at microwave and radio frequencies suggest a different spectral power-law for the CR e^\pm at ~ 1 GeV [56, 58, 76] compared to CR e^\pm flux measurements at higher energies [4, 81]. While changes in the spectral power-law describing these components are motivated by the reasons just described, sharp breaks used to implement them are theoretically less accurate and fit slightly worse the AMS positron fraction spectrum.

In addition, our physically motivated models include the impact of solar modulation by using the force field approximation. Solar modulation modifies the position and normalization of the dark matter signal flux, but is negligible at energies > 5 GeV.⁴ We do not expect solar

³ At a few GeV the e^\pm energy losses due to bremsstrahlung emission, dominant at lower energies, equal locally those due to synchrotron radiation and ICS (dominant at higher energies). Since the energy loss rate dE/dt due to bremsstrahlung radiation scales as E while the dE/dt due to synchrotron and ICS as E^2 (at the Thompson cross-section regime), a spectral change in the propagated e^\pm around that energy is expected (see, e.g., Ref [56]).

⁴ In certain models, solar modulation can also affect the observed

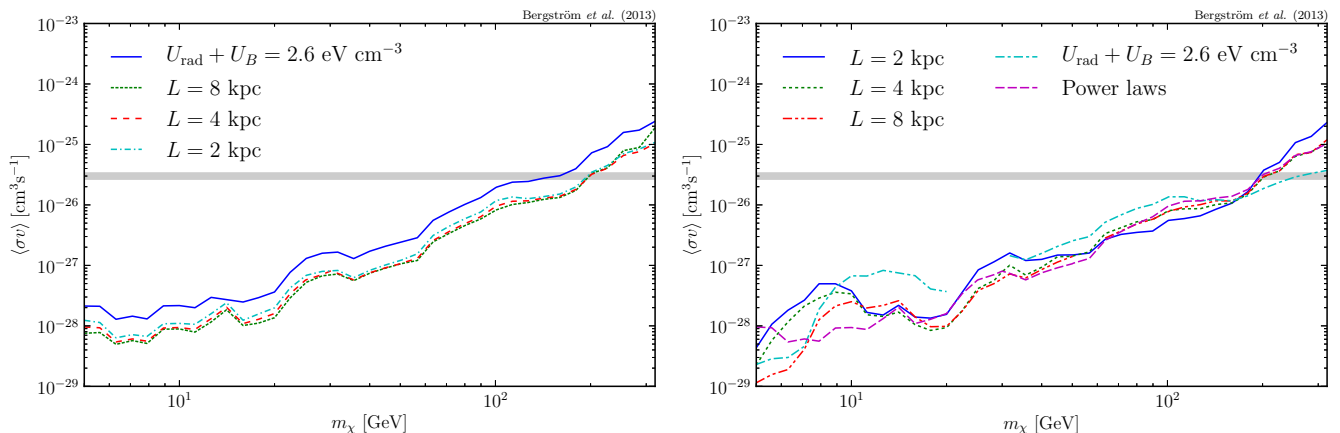


FIG. 4. *Left panel:* Limits obtained when different propagation models for the DM signal are adopted, using the power-law background model adopted in the main text. *Right panel:* Limits derived using different, physically motivated, background models. In both frames, the results are for the case of DM annihilations to e^+e^- . If not stated otherwise, we adopt the benchmark values for $L = 4$ kpc and the local radiation plus magnetic field density 1.7 eV cm^{-3} .

modulation to significantly smoothen a sharp spectral peak at higher energies.

Given that we consider a population of pulsars as one possible source of the rising positron fraction above 10 GeV (with TeV-scale DM or a single dominant pulsar being alternative possibilities), we will briefly discuss the impact of their modeling on our limits. For pulsars that eventually inject equal amounts of e^\pm into the ISM, their injection spectra can be estimated from gamma-ray and synchrotron observations towards known pulsars, such as the Crab.⁵ Typical injection power-law values for the differential spectrum are expected to be in the range of 1-2 leading to propagated spectra with power-laws in the range of 2.0 ± 0.5 . Our fits for the averaged pulsar contribution agree with these expectations.

In addition, as suggested by Refs. [85–87], the total contribution from many pulsars – each with a different age, distance, initial rotational energy, injected energy into e^\pm , and unique environmental surroundings affecting energy losses and diffusion – is expected to give a spectrum with many peaks and dips, especially at higher energies where fewer pulsars significantly contribute. With fine enough energy resolution and high statistics, one should be able to observe such spectral features. By using the data from the ATNF pulsar catalogue [88] and

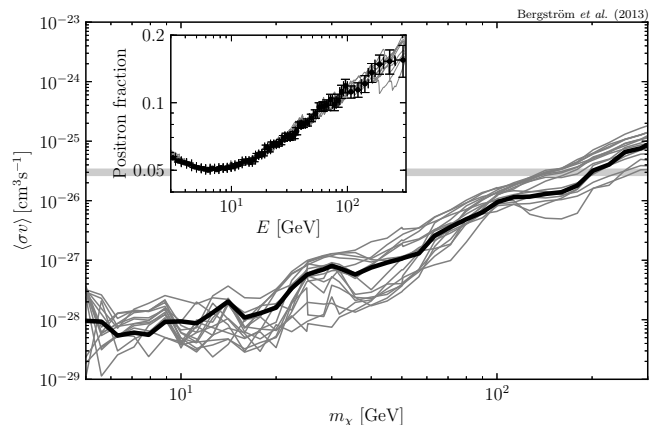


FIG. 5. The *black line* shows our nominal limit on e^+e^- final states, obtained by adopting the power-law background model. The *gray lines*, in contrast, show limits obtained when the contribution from many pulsars is taken into account (for 15 different realizations).

implementing the parametrization of Ref. [85], we ran multiple realizations of such combined spectra to study the impact of possible dips and peaks in the background spectrum on the derived DM limits. In particular, we include in these realizations all pulsars within 4 kpc from us, except for millisecond pulsars and pulsars in binary systems. While we keep their individual locations and ages in all realizations fixed, we vary i) the local CR diffusion properties and energy-losses, ii) the cuts on the current spin-down power of pulsars as recorded in the ATNF catalogue and, most importantly, iii) the fraction η of initial rotational energy of the individual neutron stars that is injected into the ISM in the form of e^\pm .

We then fit to the AMS data the injection spectral

height of the peak in the positron fraction by changing the ratio of electrons-to-positrons of same energy before entering the Heliosphere [52, 82].

⁵ Yet the uncertainties are still large due to a lack of exact understanding of local environments or the type of relevant supernova remnants (within which the pulsars exist); typically, the e^\pm also get further accelerated at the termination shock between the magnetosphere and the pulsar wind nebulae (PWN), and the e^\pm injected to the ISM are dominantly coming from middle aged pulsars after their respective PWN have been disrupted (see Refs. [83–85])

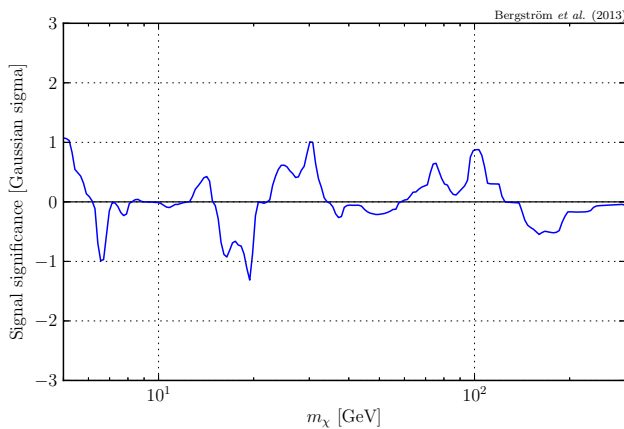


FIG. 6. Significance for a contribution from a e^+e^- DM signal to the AMS-02 positron fraction, for different DM energies, in units of Gaussian sigma. Negative values correspond to negative (but unphysical) signal normalizations.

properties (taken to be the same for all pulsars), the *averaged* value of η , the primary SNe e^- , secondary e^\pm CR flux normalizations and the solar modulation potential. Even though the injection e^\pm spectrum is taken to be the same for simplicity, however, the propagated pulsar spectra differ because of the different ages, distances and energy outputs; this is clearly seen in the inset of Fig. 5 where we plot the resulting positron fraction. For

DM channels that give broad continuous spectra, such as muons and taus (see Fig. 1), the presence of multiple peaks and dips is unimportant. For hard spectra such as from monochromatic e^\pm , however, our limits can be modified by a factor of up to ~ 3 , as also shown in Fig. 5.

In Fig. 6 we show, for the case of e^+e^- final states, the local significance for a DM signal as function of the DM mass. The significance is plotted in units of Gaussian sigma, and given by the square-root \sqrt{TS} of the Test Statistics $TS = -2 \log \mathcal{L}_{\text{null}}/\mathcal{L}_{\text{alt}}$. Here, $\mathcal{L}_{\text{alt}/\text{null}}$ denote respectively the likelihood of the alternative (DM signal) and null (no DM signal) hypothesis. For illustration, we also allow negative (obviously unphysical) signal normalizations in the fit, which are mapped onto the negative y-axis. As background model in the fit we use the reference power-law model from Ref. [2]. We do not find any indications for local, edge-like, features in the AMS data.

Lastly, as a simple cross-check, we have also run DarkSUSY [89] with standard parameters for propagation (based on the prescription given in Ref. [32]) and an NFW profile normalized to 0.4 GeV cm^{-3} . For the electron spectrum, we used a simple broken power law which agrees with the PAMELA electron data [81] for $E > 5 \text{ GeV}$. Knowing that the AMS positron fraction measurement is well described by a simple background model, we then just demand that the DM signal does not exceed the reported 2σ error bars at the energy of the feature. The resulting limit curve agrees well with the more sophisticated treatment described in the main text.